

2007-12-27 00:12

TO:MSAL (Queller)

FROM:IKEUCHI,SATO &amp; PARTNERS PATENT

T-613 P.004/013 F-308



ELSEVIER

Journal of Crystal Growth 196 (1999) 47–52

JOURNAL OF  
CRYSTAL  
GROWTH

## Synthesis of gallium nitride by ammonia injection into gallium melt

M. Shibata\*, T. Furuya, H. Sakaguchi, S. Kuma

Advanced Research Center, Hitachi Cable Ltd., 3350 Kidamari-cho, Tsukuba-shi, Ibaraki, 300-0026, Japan

Received 14 March 1998; accepted 25 June 1998

### Abstract

Gallium nitride (GaN) was synthesized by injecting ammonia gas into molten gallium at 900–980°C under atmospheric pressure. A large amount of GaN powder was reproducibly obtained using a simple apparatus. The synthesized powder was characterized by scanning electron microscopy, X-ray diffraction, photoluminescence and energy dispersive X-ray spectroscopy, and was found to consist of fine crystals of hexagonal GaN of good quality. The total of GaN obtained was far more than the amount calculated from expected saturation solubility in the Ga melt at that temperature. We speculate that the GaN crystals were largely formed by direct reaction between Ga and the gaseous N source at the surface of the NH<sub>3</sub> bubbles in the melt. GaN synthesized by this method may be useful as a starting material for bulk growth. © 1999 Elsevier Science B.V. All rights reserved.

PACS: 81.05; 81.70; 81.10; 81.20.E

Keywords: Gallium nitride; Synthesis; Injection method

### 1. Introduction

Gallium nitride (GaN) and its related compounds have begun to be used in optoelectronic devices operating in the band from blue to ultraviolet wavelength [1–3]. GaN and its related crystals are usually grown by metallorganic vapor-phase epitaxy (MOVPE) or by molecular beam epitaxy (MBE). The reliability of optoelectronic

devices depends on the quality of epitaxial layers and many efforts have been made to reduce the dislocations and other defects in these layers [3,4]. One big problem which has not yet been solved, however, is heteroepitaxial growth. GaN is generally grown on sapphire or silicon carbide (SiC) substrates, because bulk single crystals of group III nitrides with dimensions adequate for substrate are not obtainable. The heteroepitaxial growth causes defects due to lattice mismatch as well as thermal expansion coefficient difference. Thus, there is a strong need for the development of bulk GaN crystals.

\* Corresponding author. Fax: +81 298 26 6411; e-mail: shibata@arc.hitachi-cable.co.jp.

2007-12-27 09:12

TO:HSL (Aveller)

FROM:IKEUCHI,SATO &amp; PARTNERS PATENT

T-613 P.005/013 F-308

48

M. Shibata et al / Journal of Crystal Growth 196 (1999) 47-52

Several papers about basic studies on GaN crystal growth were published in the period 1970-1980 [5-10]. Nowadays, though GaN substrates are required, a few studies on bulk GaN growth are found in the literature [11-13], while there are many reports on epitaxial growth. There has also been little study of synthesis of GaN as a raw material for bulk crystal growth. Gallium (Ga) metal and nitrogen gas ( $N_2$ ) do not react under atmospheric pressure and ammonia gas ( $NH_3$ ) is used as a nitrogen source in many cases. There are several reports on synthesis in the early stage of GaN development by heating the Ga metal contained in a quartz (or graphite, boron nitride) boat in a  $NH_3$  atmosphere [14-18]. This method using a Ga container boat, however, yields less synthesis, because a thin GaN crust forms on the Ga surface and inhibits further reaction between Ga and  $NH_3$ . Other synthesis methods have recently been reported, for instance, an ammonothermal method [19] which uses high pressure, and a plasma assisted method [20,21]; but these techniques require special equipment such as a high-pressure autoclave and a plasma generator, respectively.

In this study, an injection method to synthesize GaN was investigated. A similar method was applied for synthesis of indium phosphide (InP) crystals by injection of phosphorus vapor into molten indium [22]. By injecting ammonia gas into molten Ga, it is possible to obtain a large amount of GaN powder under atmospheric pressure with a simple furnace.

## 2. Experimental procedure

Fig. 1 shows a schematic drawing of the experimental apparatus for GaN synthesis. A quartz vessel which contains molten Ga is put in a resistive heating furnace. The vessel has a quartz pipe with inner diameter of 6 mm for  $NH_3$  injection into the melt which can move vertically in the vessel while retaining the gas seal. Boron nitride plates in the vessel above the melt reflect heat radiation from the melt. The temperature of synthesis is monitored using a thermocouple inserted into the melt and is feedback-controlled by the heater. All processes

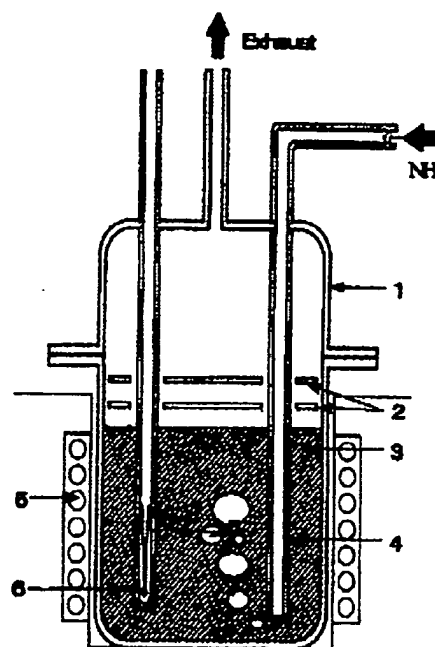


Fig. 1. Schematic drawing of apparatus for GaN synthesis: (1) quartz vessel, (2) radiation reflectors made of BN, (3) molten Ga, (4) injection pipe, (5) resistive heater, (6) thermocouple

during the synthesis were performed under atmospheric pressure.

5N Ga of 2500-4000 g was charged in the vessel. Initially, the injection pipe was held above the melt and  $H_2$  gas of 4N was introduced into the vessel through the pipe. Ga was heated in a flowing  $H_2$  atmosphere to remove the gallium oxide covering the melt surface. When the melt temperature had reached 900-980°C, the injection pipe was inserted into the melt. Depth of the Ga melt was about 6-9 cm and the end of the pipe was kept about 1 cm above the bottom of the vessel. Then, the gas which was led through the injection pipe was replaced by 5N  $NH_3$ .  $NH_3$  gas was injected into the melt at a rate of 100-200  $cm^3/min$ . The injected gas made bubbles and reacted with Ga melt as it rose through the melt. The injection was carried out for 4.5-7.5 h, after which the pipe was withdrawn from the melt and the heater was extinguished to allow the furnace to cool down. After the

2007-12-27 00:12

TO: HSMR (Muller)

FROM: IKEYUCHI, SATO &amp; PARTNERS PATENT

T-613 P.008/013 F-308

M. Shibata et al. / Journal of Crystal Growth 196 (1999) 47–52

49

pipe was withdrawn, it continued to emit  $\text{NH}_3$  gas, and an  $\text{NH}_3$  atmosphere was retained in the vessel until the temperature of the furnace dropped enough that it would not decompose the GaN.

Fine GaN powder was synthesized and floated up in the Ga melt. The surface of the melt became muddy, because the powder was mixed with unreacted Ga. To separate the powder from the muddy melt, the remaining Ga was washed out with a mixture of hydrochloric acid (HCl) and hydrogen peroxide solution ( $\text{H}_2\text{O}_2$ ), and then the powder was filtered. The obtained GaN powder was washed with pure water and dried in air for several days.

The GaN powder was observed by scanning electron microscopy (SEM) and characterized by X-ray diffraction (XRD), photoluminescence (PL), energy dispersive X-ray spectroscopy (EDX) and X-ray fluorescence analysis (FXA).

### 3. Results

#### 3.1. Synthesis of GaN

We have performed several runs of synthesis. The experimental conditions of synthesis and respective results are summarized in Table 1. It is difficult to

measure accurately the amount of GaN powder synthesized in an experiment, because it is obtained in a muddy state as described earlier. We usually spooned out only the muddy surface of the melt and separated the powder from it. Most of the Ga melt which still included some GaN powder remained in the vessel after spooning, and this was recharged for the next synthesis. Some powder might be lost through the separation process. Therefore, we measured the vessel weight including the melt before and after injection and found the difference. Assuming the weight increase of the vessel was due to reacted nitrogen atoms, the total weight of synthesized GaN was calculated. For example, in condition No. 1, about 40 g of dark gray GaN powder was obtained from the "mud" and the calculated weight of synthesized GaN was 70 g.

#### 3.2. Characterization of GaN powder

SEM photographs of the obtained GaN powder are shown in Fig. 2. It is composed of fine crystals  $\sim 10 \mu\text{m}$  in size. These crystals aggregate and form clusters. The crystals are of several shapes; many are like porous pumice and others show various hexagonal habits of GaN, like needles, plates and so on. The typical needle-like crystals are shown in Fig. 2b.

Table 1  
Synthesis conditions and results

Synth. No	Ga charge (g)	Synth. Temp. ( $^{\circ}\text{C}$ )	$\text{NH}_3$ injection rate ( $\text{cm}^3/\text{min}$ )	Injection period (hr)	Weight increase* (g)	GaN increase* (g)	Efficiency of reaction* (%)
1	4000	980	200	7.5	11.8	70.5	21.0
2	3400	930	200	6.5	17.5	104.6	35.9
3	2700	900	100	6	4.1	24.5	18.2
4	3500	900	150	6.0	6.9	41.2	20.4
5	3500	900	200	4.5	5.3	31.7	15.7
6	3500	900	200	4.5	5.4	32.3	16.0
7	3500	900	200	4.5	5.3	31.7	15.7
8	2500	950	200	4.5	11.1	66.3	32.9
9	2500	950	200	4.5	8.3	49.6	24.6

\*weight increase refers to the difference in vessel weight containing the Ga melt before and after  $\text{NH}_3$  injection

\*GaN increase means the sum of synthesized GaN calculated from the value of weight increase, assuming that the increased weight is all due to reacted nitrogen.

\*efficiency of reaction means the amount of reacted  $\text{NH}_3$ , divided by that injected, calculated by weight increase,  $\text{NH}_3$  injection rate and injection period.

2807-12-27 00:12 TO-HS&amp;L (Aueller)

FROM: KUCHI, SATO &amp; PARTNERS PATENT

T-813 P.007/013 F-308

50

M. Shubam et al. / Journal of Crystal Growth 196 (1999) 47-52

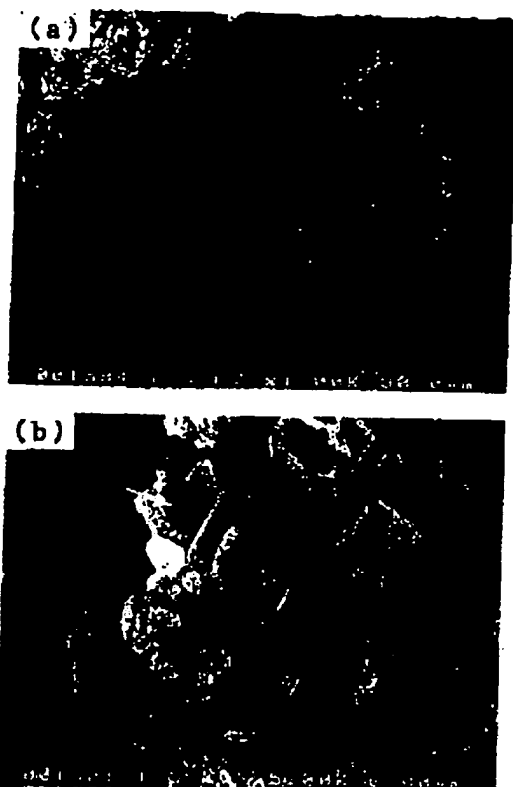


Fig. 2. (a) SEM image of the synthesized GaN powder which consists of various shaped crystals. (b) some component crystals show hexagonal habit of GaN. Arrows indicate the typical needle-like crystals.

The GaN powder was characterized by XRD using Cu K $\alpha$  radiation. Fig. 3 shows a typical XRD pattern of the powder in  $\theta$ - $2\theta$  scan mode. The peak profile corresponds well with that of the hexagonal GaN reported in the X-ray powder data file of ASTM. The peaks are slightly broadened, perhaps because the powder includes very fine crystallites of  $\sim 0.1 \mu\text{m}$ .

PL spectra of the GaN powder were measured at room temperature using a He-Cd laser excitation source. A typical PL spectrum is shown in Fig. 4. A strong band-edge emission peak of 363 nm is observed without any deep level luminescence.

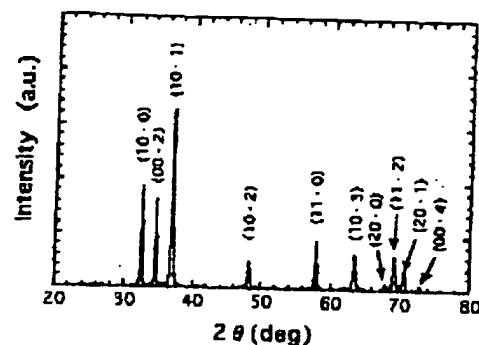


Fig. 3. Typical XRD pattern of the GaN powder using Cu K $\alpha$  radiation.

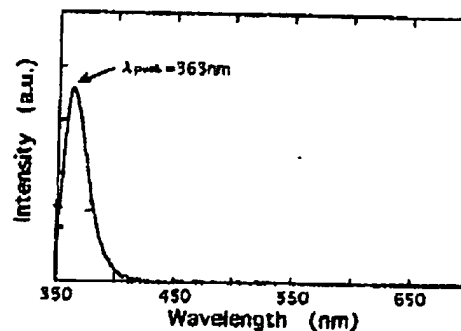


Fig. 4. Typical PL spectrum of the GaN powder measured at room temperature.

A qualitative analysis was done by EDX. Peaks corresponding to Ga and N were detected, but no other impurity could be found. From these results, the synthesized powder was recognized as high-quality GaN.

#### 4. Discussion

##### 4.1. Mechanism of synthesis

In the conventional injection method, the source melt is initially heated up to the melting point of the

2007-12-27 00:12

TO-HSUL (Aeller)

FROM-IKEUCHI, SATO &amp; PARTNERS PATENT

T-613 P.008/013 F-308

*M. Shibata et al / Journal of Crystal Growth 196 (1999) 47-52*

51

target compound and then the melt of the compound is made by injection. The target compound crystal is generated by cooling down from its own melt. In this report, GaN fine crystals were obtained far below the melting temperature of GaN. The total amount of synthesized GaN powder was far greater than the amount of GaN calculated from saturation solubility in the Ga melt at that temperature. For example, a solubility of  $3 \times 10^{-5}$  mol fraction of GaN in Ga melt at 1150°C has been reported [7]. Using this value, 4000 g Ga melt allows to dissolve only 0.14 g GaN at 1150°C. We estimate that 70 g of GaN was synthesized in 4000 g Ga melt at 980°C, as described above. Precipitation from the solution during the injection process may not have been dominant, because of the small solubility of GaN at that temperature and of the small temperature difference in the melt. The surface of the melt gradually became viscous during  $\text{NH}_3$  injection, suggesting that the crystals of GaN must be generated during the injection. The generation of the GaN crystals coincides with the reaction between Ga and  $\text{NH}_3$ . We speculate that most of the crystals are formed directly from Ga and the gaseous N source ( $\text{NH}_3$  may be decomposed prior to reaction into radical form) on the surface of  $\text{NH}_3$  bubbles in the melt. During their rise to the melt surface, the bubbles are constantly changing in shape and make a new interface with the melt. Synthesized GaN at the interface does not prevent further reaction, and this is the reason only fine particles are created.

The efficiency of the reaction in this method depends on the synthesis temperature as shown in Table 1. This suggests that the decomposition rate of  $\text{NH}_3$  limits this efficiency. Decrease of the efficiency above 930-950°C is believed to be due to increasing decomposition of synthesized GaN. The yield of GaN is limited by the amount of  $\text{NH}_3$  injected and not the amount of charged Ga. The Nos. 5-7 series of synthesis experiments in Table 1 confirms that reproducibility can be achieved by this method.

Crystalline structure of the synthesized GaN is shown by XRD patterns to be hexagonal. This concurs with a report that MOVPE growth of GaN shows a structural transition associated with cubic to hexagonal at around 750°C [23]. Our experi-

mental temperature, above 900°C, was evidently high enough to form hexagonal crystals.

#### 4.2. Purity of the GaN powder

Impurities were also analyzed by FXA. Contamination of Si had been thought to originate in the quartz vessel and injection pipe, but no Si was detected there (detection limit: < 0.001 mass%). Other remarkable elements (Mg, Al, Zn, Mn, Fe, Ni, Cr, Cu, Zr and Cl) were not detected or, if detected, were under 0.01 mass%. The purity of the powder was estimated at about 99.9%.

The synthesized GaN powder was obtained in a mixture with Ga melt. The separation process is very important to get high purity GaN. When the separation is incomplete, unreacted Ga remains with the powder and is easily oxidized during the separation and/or the drying process. The porous structure of the synthesized GaN powder makes it difficult to remove the remaining Ga, and also to dry the powder. Therefore, the impurity O was sometimes detected by EDX measurement. If gallium oxide ( $\text{Ga}_2\text{O}_3$ ) is formed, it can be observed by SEM as tiny dots of  $\sim 1 \mu\text{m}$  on the surface of GaN fine particles as shown in Fig. 5.  $\text{Ga}_2\text{O}_3$  can be easily removed by HCl treatment of the powder or by ammonolysis at 930°C.



Fig. 5. SEM image of Ga oxides on the surface of GaN crystals which was obtained by an insufficient separation process. Ga oxides are observed like dots as indicated by arrows.

2007-12-27 00:13

TO-HSML (Kuehler)

FROM-KEUCHI, SATO &amp; PARTNERS PATENT

T-613 P.000/013 F-308

52

*M. Shibata et al. / Journal of Crystal Growth 196 (1999) 47-52*

## 5. Conclusions

In our study of a synthesis method of GaN by injecting  $\text{NH}_3$  gas into molten Ga, a large amount of GaN powder was synthesized reproducibly at 900–980°C under atmospheric pressure with a simple apparatus. Synthesized GaN powder was obtained as a mixture with unreacted Ga. Separated GaN powder was observed by SEM and found to consist of fine crystals of  $\sim 10 \mu\text{m}$ . The powder was characterized by XRD and recognized as hexagonal GaN. PL spectrum was also measured at room temperature and only a strong band-edge emission of GaN was observed. The obtained powder was analyzed by EDX and FEA and found to be composed of high purity GaN.

The amount of GaN obtained was far in excess of the expected amount of that calculated from saturation solubility in the Ga melt. The efficiency of the synthesis reaction depended on the temperature, which means that the decomposition rate of  $\text{NH}_3$  limits the yield of synthesis. Based on these findings, we suggest that the GaN crystals were largely formed by direct reaction between Ga and the gaseous N source at the surface of the  $\text{NH}_3$  bubbles in the melt.

The authors believe that GaN synthesized by this method is a useful starting material for bulk growth.

## References

- [1] S. Nakamura et al., Proc. 2nd Int. Conf. on Nitride Semiconductors, Tokushima, S-1, 1997, p. 444.
- [2] A. Kuramata et al., Jpn. J. Appl. Phys. 36 (1997) L1130.
- [3] S. Nakamura et al., Jpn. J. Appl. Phys. 36 (1997) L1568.
- [4] A. Usui et al., Jpn. J. Appl. Phys. 36 (1997) L899.
- [5] C.D. Thurmond, R.A. Logan, J. Electrochem. Soc. 119 (5) (1972) 622.
- [6] V.S. Ban, J. Electrochem. Soc. 119 (6) (1972) 761.
- [7] R.A. Logan, C.D. Thurmond, J. Electrochem. Soc. 119 (12) (1972) 1727.
- [8] M. Hlegans, J. Crystal Growth 13/14 (1972) 360.
- [9] T.L. Chu et al., J. Electrochem. Soc. 121 (1) (1974) 160.
- [10] R. Madar et al., J. Crystal Growth 31 (1975) 197.
- [11] S. Porowski, J. Crystal Growth 166 (1996) 583.
- [12] S. Kurai et al., Jpn. J. Appl. Phys. 35 (1996) L77.
- [13] Yu.A. Vodakov et al., J. Crystal Growth 183 (1998) 10.
- [14] W.C. Johnson, J.B. Parsons, M.C. Crew, J. Phys. Chem. 36 (1932) 2651.
- [15] I.G. Pichugin, D.A. Yashov, Neorg. Mater. 6 (1970) 1973.
- [16] R.B. Ziemerhorn, J. Mater. Sci. 5 (1970) 1102.
- [17] E. Ejder, J. Crystal Growth 22 (1974) 44.
- [18] D. Elwell et al., J. Crystal Growth 66 (1984) 45.
- [19] R. Dwilinski et al., Acta Phys. Pol. A 88 (1995) 833.
- [20] H.D. Li et al., Appl. Phys. Lett. 69 (1996) 1285.
- [21] A. Argolia et al., Appl. Phys. Lett. 70 (1997) 179.
- [22] For example: D.J. Dowling et al., J. Crystal Growth 87 (1988) 137.
- [23] H.C. Liu et al., Jpn. J. Appl. Phys. 36 (1997) L598.

2007-12-27 00:13

TO-HSUL (Aeller)

FROM-IKEUCHI, SATO &amp; PARTNERS PATENT

T-513 P.010/013 F-308

64

## LETTERS

# Congruent melting of gallium nitride at 6 GPa and its application to single-crystal growth

WATARU UTSUMI\*, HIROYUKI SAITO, HIROSHI KANEKO, TETSU WATANUKI, KATSUTOSHI AOKI AND OSAMU SHIMOMURA

Synchrotron Radiation Research Center, Japan Atomic Energy Research Institute, Mikazuki-cho, Sayo-gun, Hyogo 679-5148, Japan  
\*w-utsu@spring8.or.jp

Published online: 26 October 2007; doi:10.1038/nature06003

**T**he synthesis of large single crystals of GaN (gallium nitride) is a matter of great importance in optoelectronic devices for blue-light-emitting diodes and lasers. Although high-quality bulk single crystals of GaN suitable for substrates are desired, the standard method of cooling its stoichiometric melt has been unsuccessful for GaN because it decomposes into Ga and N<sub>2</sub> at high temperatures before its melting point. Here we report that applying high pressure completely prevents the decomposition and allows the stoichiometric melting of GaN. At pressures above 6.0 GPa, congruent melting of GaN occurred at about 2,220 °C, and decreasing the temperature allowed the GaN melt to crystallize to the original structure, which was confirmed by *in situ* X-ray diffraction. Single crystals of GaN were formed by cooling the melt slowly under high pressures and were recovered at ambient conditions.

Blue-light-emitting devices are usually fabricated by epitaxial growth on sapphire substrates because large single crystals of GaN are unavailable. However, there is a large mismatch in the lattice constants of sapphire and GaN. This mismatch causes high-density dislocations in the deposited layer and is a major obstacle for improving device quality. The production of large single crystals of GaN, several inches in diameter, that are suitable as substrates is therefore desirable. Because standard Czochralski or Bridgman growth cannot be used because of the decomposition problem, other attempts have been made to obtain single crystals of GaN, such as hydride vapour-phase epitaxy<sup>1</sup>, the Na flux method<sup>2</sup> and laser heating with a diamond anvil cell<sup>3</sup>. But all have been unsuccessful in growing large single crystals suitable as substrates for optoelectronic devices. For the application of high pressure, a Polish group has conducted extensive studies with their high-pressure gas apparatus and has successfully obtained thin plates of GaN single crystals<sup>4–6</sup>. However, the maximum pressure (2 GPa) in their gas apparatus was not high enough to prevent decomposition completely. Their method for growing GaN crystals was therefore based not on cooling a GaN melt but on the absorption of high-pressure N<sub>2</sub> gas to a Ga melt under the pressure and temperature conditions at which solid GaN is stable. Our new approach is to use a large-volume multi-anvil high-pressure apparatus that can generate much higher pressures and temperatures. The first observation of congruent melting in GaN was confirmed by *in situ* X-ray diffraction under high pressures and temperatures, and single crystals of GaN from its stoichiometric melt were recovered at ambient conditions.

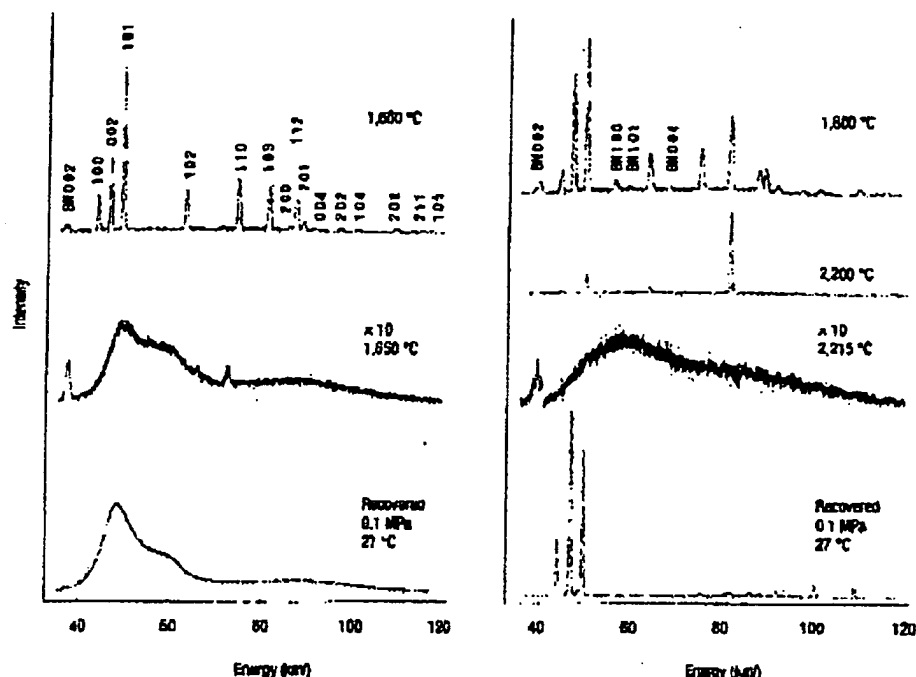
*In situ* X-ray diffraction experiments were performed using the SMAP, a multi-anvil high-pressure apparatus for synchrotron radiation, installed on beamline BL14B1 (bending magnet source) at the SPring-8 site in Harima Science Garden City, Japan<sup>7</sup>. Figure 1a shows the variations in the X-ray diffraction profiles with increasing temperature at 2.0 GPa. The starting material was a high-purity (99.99%) powder of GaN (Kojundo Chemical Laboratory, Saitama, Japan). The sample maintained its original wurtzite structure at 1,600 °C (extra peaks from the BN capsule are also shown). At 1,650 °C all sharp peaks from GaN disappeared completely and a continuous broad diffraction profile was observed, which indicated that GaN completely decomposed and a Ga melt formed. This decomposition temperature of 1,650 °C at 2.0 GPa is consistent with the previous study, which used high-pressure gas apparatus<sup>8</sup>. The sample recovered at ambient conditions showed a similar broad diffraction profile, which was confirmed to be Ga melt by comparing the profile with that of the reagent Ga. In contrast, GaN melted congruently at 6.0 GPa (Fig. 1b). Clear diffraction profiles of wurtzite structure were observed up to 1,800 °C. When the temperature was greater than 1,800 °C, anomalous variation of the peak intensity occurred and some peaks were unobservable because of the grain growth of the sample<sup>9</sup>, but all observed diffraction peaks could be indexed as the wurtzite structure of GaN (and hexagonal BN), indicating that the sample was still in a solid phase. At 2,215 °C, all of the sharp peaks from the GaN crystal vanished and a broad diffraction profile appeared. In this profile, the shape and energy of the first sharp diffraction peak were significantly different from those of Ga melt, which suggests that the GaN melted congruently at this temperature. After melting was confirmed, turning off the power to the furnace rapidly decreased the temperature; the pressure was then released. The diffraction pattern of the recovered sample was obtained under ambient conditions and showed that it was a polycrystal of wurtzite structure. This indicates that, unlike at 2.0 GPa, the melt formed at 6.0 GPa crystallized to the original structure when the temperature was decreased.

The pressure-temperature diagram (Fig. 2) summarizes the decomposition and melting behaviour of GaN. The experiments were performed for different pressures (4.0, 5.0, 5.5, 6.4 and 6.9 GPa) to determine the temperature at which each event occurred. At pressures less than 5.5 GPa, GaN decomposed into Ga and N<sub>2</sub> and the decomposition temperature increased almost linearly with pressure.

DOI: 10.1038/nature06003 | VOL 21 | NOVEMBER 2007 | www.nature.com/nature

798

©2007 Nature Publishing Group



(solid circles). In contrast, at 6.4 and 6.8 GPa (the maximum pressure in the present apparatus with the same-size anvils) congruent melting occurred at 2,225 °C, which is close to the temperature at 6.0 GPa (solid triangles). Figure 2 shows clearly that the decomposition temperature increases rapidly with pressure, whereas the pressure dependence of the melting temperature is negligible. Consequently, the decomposition temperature exceeds the melting temperature at about 6.0 GPa and congruent melting occurs at higher pressures. The unit-cell volume of solid GaN just before melting, calculated from the *in situ* diffraction profile is 45.56 Å<sup>3</sup>, almost equal to the initial value at ambient conditions (45.52 Å<sup>3</sup>). The Clausius-Clapeyron equation,  $dT/dP = \Delta V/\Delta S$ , indicates that the volume change on melting or solidification must be very small because the slope of the melting line is almost zero. There should be an additional phase boundary (thick dashed line in Fig. 2) between Ga + 1/2 N<sub>2</sub> and GaN (liquid), which was not determined experimentally by the present study. It is likely that this boundary has a negative slope because the solubility of N<sub>2</sub> in Ga melt increases with pressure<sup>24</sup>. Further experiment is needed to confirm this hypothesis. According to the calculation by Van Vechren<sup>25</sup>, the melting temperature of GaN at 6.0 GPa is 2,403 °C and the melting line has a very small negative slope (-19.1 °C/GPa) (thin dotted line). The present experimental results are consistent with this theory, which is good considering that the calculation was made 30 years ago. A decomposition

An experiment for single-crystal growth was performed at 6.8 GPa. In the same manner as in the first experiment, powdered GaN was placed in a BN capsule (inner diameter 1.0 mm, height 1.0 mm) and compressed in the multi-anvil apparatus. Temperature during growth increased to 2,300 °C, which was high enough for molten; it was then slowly decreased to 2,100 °C at a constant rate of 1 °C/min.<sup>10</sup> After the temperature was further decreased to room temperature (30 °C min<sup>-1</sup>), the pressure was released. The BN capsule recovered at ambient conditions was filled with many pieces of transparent GaN single crystals with a slightly yellowish colour. A scanning electron micrograph of the obtained GaN single crystals is shown in Fig. 3. The average crystal size obtained in the present study was about 100 µm. Figure 4 is an X-ray oscillation photograph of the recovered GaN single crystal. All Bragg spots can be indexed as a unit



## LETTERS

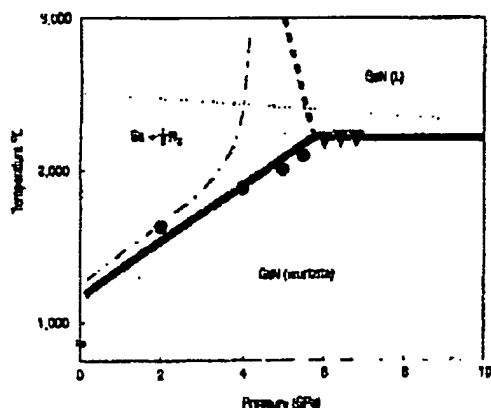


Figure 2 Phase diagram of GaN under high pressure and temperature. Solid circles and triangles denote the pressure and temperature conditions at which GaN decomposed and congruent melting occurred, respectively. The decomposition temperature increased almost linearly with pressure. Congruent melting occurred above 6 GPa and the pressure dependence of the melting temperature was very small. The thick dashed line is a hypothetical phase boundary between  $\text{Ga} + 1/2\text{N}_2$  and GaN (liquid). The thin dashed line is the melting line calculated in ref. 10, and the thin dotted line is the decomposition line from ref. 9).

cell of the wurtzite structure, and no extra spots were observed. Although a very small divergence beam from the undulator device was used, all spots were very sharp without any peak splitting, which is good evidence of the high crystallinity of the GaN crystal obtained. The Raman spectrum of the specimen was also measured and it showed sharp peaks at wavenumbers of 567 and 734  $\text{cm}^{-1}$ , corresponding to the  $E_2$  and  $A_1$  (LO) phonon modes, respectively, of the wurtzite structure of GaN. Further characterizations are now in progress.



Figure 3 Scanning electron micrograph of the GaN single crystals obtained by laser cooling of the stoichiometric melt at 6.6 GPa.

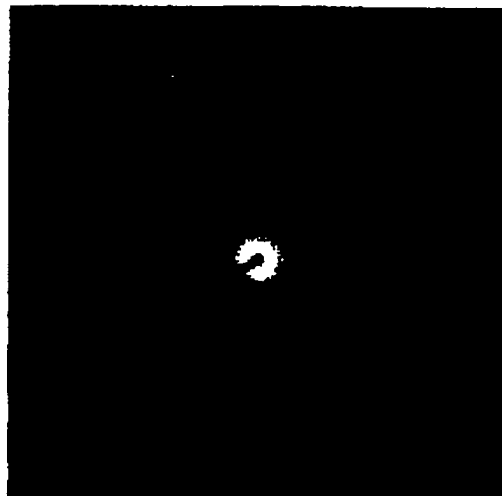


Figure 4 X-ray diffraction photograph of the recovered GaN single crystal. The image was taken with a four-circle diffractometer and an imaging plate installed on beamline BL22XU at the SPring-8 site. The X-ray source was an undulator device, the X-rays were made monochromatic with a Si double-crystal monochromator. The X-ray energy was 25 keV and the crystal-to-film distance was 184.27 mm. The incident X-ray beam was perpendicular to the  $h^*k^*$  plane of the crystal, and the detection angle was  $\approx 10^\circ$  around the  $c^*$ -axis.

These results strongly suggest the possibility of synthesizing a large single crystal of GaN from a stoichiometric melt at high pressures. A pressure of 6 GPa, the critical value for the congruent melting of GaN, is almost the same as that necessary to transform graphite into diamond with metal solvent catalysts. Various large-scale high-pressure presses are now commonly operated in the industrial production of synthetic diamond, and large sintered diamond compacts with diameters as large as 100 mm are already commercially available. By applying the established high-pressure technology, we expect large single crystals of GaN several centimeters long to be synthesized without serious technical difficulties.

## METHODS

Crystals of high-purity GaN were synthesized with a cubic apparatus and apparatus (CMAF) installed on beamline BL22XU at the SPring-8 site. Polycrystalline GaN with a size of 1 mm  $\times$  1 mm were used as starting materials, and the high-pressure cell assembly in the present study was a modification of that used in our previous study<sup>9</sup>. GaN powder was placed in a pressure cell (1.5 mm  $\times$  1.5 mm  $\times$  1.5 mm) and GaN with a length of 1 mm was placed in a separate block of polycrystalline diamond. The temperature was measured by a PtRh (90% Pt-10% Rh) thermocouple. Because the thermocouple did not survive the high-pressure cell, the temperature was estimated about 1,000  $^\circ\text{C}$  by extrapolating the thermocouple response from the point of the thermocouple. The temperature was estimated to be less than  $\pm 25^\circ\text{C}$ . Incident X-rays (wavelength of 0.0481 nm) were focused on the sample, and the diffracted X-rays were measured by a  $\text{Cu}$   $\beta$ -radiation detector (scattered on a goniometer (10  $^\circ$   $\times$  20  $^\circ$  angle was fixed at  $90^\circ$ ). Pressure values were based on the pressure calibration curve of ruby (Fig. 1). The pressure was estimated by a method described in our previous study<sup>9</sup>. The pressure distribution was confirmed by measuring the volume of the sample before and after the high-pressure cell. The pressure distribution was estimated by a very high-resolution X-ray diffraction method. The pressure was estimated to be less than  $\pm 0.5$  GPa and about 2,000  $^\circ\text{C}$ .

2007-12-27 00:14 TO: HSHL (Buller)

FROM: IKEUCHI, SATO &amp; PARTNERS PATENT

T-613 P.013/013 F-308

**LETTERS**

Received 27 July 2003; accepted 23 September 2003; published 26 October 2003

**References**

1. Kato, M. K. et al. Large low-velocity core structures by hydrostatic pressure and temperature. *Earth Planet. Sci. Lett.* 112, 117-121 (1993).
2. Kato, M., Maruyama, M., Nakaguchi, T. & Okada, P. Morphology and characteristics of low-velocity core structures. *J. Geophys. Res.* 104, 10,111-10,121 (1999).
3. Nakaguchi, M. & Kato, T. Growth of subducting slabs and the low-velocity core structures. *J. Geophys. Res.* 104, 10,121-10,131 (1999).
4. Nakaguchi, M. & Kato, T. Growth of subducting slabs and the low-velocity core structures. *J. Geophys. Res.* 104, 10,131-10,141 (1999).
5. Nakaguchi, M. & Kato, T. Growth of subducting slabs and the low-velocity core structures. *J. Geophys. Res.* 104, 10,141-10,151 (1999).
6. Nakaguchi, M. & Kato, T. Growth of subducting slabs and the low-velocity core structures. *J. Geophys. Res.* 104, 10,151-10,161 (1999).
7. Nakaguchi, M. & Kato, T. Growth of subducting slabs and the low-velocity core structures. *J. Geophys. Res.* 104, 10,161-10,171 (1999).
8. Nakaguchi, M. & Kato, T. Growth of subducting slabs and the low-velocity core structures. *J. Geophys. Res.* 104, 10,171-10,181 (1999).
9. Nakaguchi, M. & Kato, T. Growth of subducting slabs and the low-velocity core structures. *J. Geophys. Res.* 104, 10,181-10,191 (1999).
10. Nakaguchi, M. & Kato, T. Growth of subducting slabs and the low-velocity core structures. *J. Geophys. Res.* 104, 10,191-10,201 (1999).
11. Nakaguchi, M. & Kato, T. Growth of subducting slabs and the low-velocity core structures. *J. Geophys. Res.* 104, 10,201-10,211 (1999).
12. Nakaguchi, M. & Kato, T. Growth of subducting slabs and the low-velocity core structures. *J. Geophys. Res.* 104, 10,211-10,221 (1999).
13. Nakaguchi, M. & Kato, T. Growth of subducting slabs and the low-velocity core structures. *J. Geophys. Res.* 104, 10,221-10,231 (1999).
14. Nakaguchi, M. & Kato, T. Growth of subducting slabs and the low-velocity core structures. *J. Geophys. Res.* 104, 10,231-10,241 (1999).
15. Nakaguchi, M. & Kato, T. Growth of subducting slabs and the low-velocity core structures. *J. Geophys. Res.* 104, 10,241-10,251 (1999).
16. Nakaguchi, M. & Kato, T. Growth of subducting slabs and the low-velocity core structures. *J. Geophys. Res.* 104, 10,251-10,261 (1999).
17. Nakaguchi, M. & Kato, T. Growth of subducting slabs and the low-velocity core structures. *J. Geophys. Res.* 104, 10,261-10,271 (1999).
18. Nakaguchi, M. & Kato, T. Growth of subducting slabs and the low-velocity core structures. *J. Geophys. Res.* 104, 10,271-10,281 (1999).
19. Nakaguchi, M. & Kato, T. Growth of subducting slabs and the low-velocity core structures. *J. Geophys. Res.* 104, 10,281-10,291 (1999).
20. Nakaguchi, M. & Kato, T. Growth of subducting slabs and the low-velocity core structures. *J. Geophys. Res.* 104, 10,291-10,301 (1999).

**Acknowledgements**

We thank M. Nakaguchi and H. Nakaguchi for their comments and useful discussions. Our thanks also go to the anonymous reviewers for their constructive comments.

**Corresponding author**

\* To whom all correspondence should be addressed. E-mail: nakaguchi@earth.riken.go.jp